

Missing Atom as a Source of Carbon Magnetism

M. M. Ugeda,¹ I. Brihuega,^{1,*} F. Guinea,² and J. M. Gómez-Rodríguez¹

¹*Departamento de Física de la Materia Condensada, Universidad Autónoma de Madrid, E-28049 Madrid, Spain*

²*Instituto de Ciencia de Materiales de Madrid, CSIC, Cantoblanco E-28049 Madrid, Spain*

(Received 24 November 2009; published 5 March 2010)

Atomic vacancies have a strong impact in the mechanical, electronic, and magnetic properties of graphenelike materials. By artificially generating isolated vacancies on a graphite surface and measuring their local density of states on the atomic scale, we have shown how single vacancies modify the electronic properties of this graphenelike system. Our scanning tunneling microscopy experiments, complemented by tight-binding calculations, reveal the presence of a sharp electronic resonance at the Fermi energy around each single graphite vacancy, which can be associated with the formation of local magnetic moments and implies a dramatic reduction of the charge carriers' mobility. While vacancies in single layer graphene lead to magnetic couplings of arbitrary sign, our results show the possibility of inducing a macroscopic ferrimagnetic state in multilayered graphene just by randomly removing single C atoms.

DOI: 10.1103/PhysRevLett.104.096804

PACS numbers: 73.20.Hb, 68.37.Ef, 72.15.Qm, 75.70.Rf

Graphite is a semimetal, where the low density of states at the Fermi level, and its high anisotropy induces significant differences from conventional metals [1]. It consists of weakly van der Waals coupled graphene layers and thus it shows a strong 2D character sharing many properties with graphene. Graphite's unusual features are enhanced in single layer graphene [2,3], where the density of states vanishes at the neutrality point, and carriers show a linear, massless, dispersion in its vicinity. In graphene, the existence of localized electronic states at zigzag edges [4,5] and vacancies [6] leads to an extreme enhancement of the spin polarizability, and model calculations suggest that magnetic moments will form in the vicinity of these defects [7–9]. It seems likely that similar phenomena also take place in other sp^2 bonded carbon materials, such as graphite. An enhanced density of states has been observed near zigzag steps in graphite surfaces [10]. The existence of these localized states suggests that magnetic moments [11–13], and possibly magnetic ordering may exist in single layer graphene and graphite. In the case of irradiated graphite, where lattice defects are expected to exist, magnetic order has been reported even at room temperature [14,15].

Introducing vacancies in graphenelike systems by irradiation has been shown to be an efficient method to artificially modify their properties [14–17]. While the role played by these vacancies as single entities has been extensively addressed by theory [6–8,18], experimental data available [14–17] refer to statistical properties of the whole heterogeneous collection of vacancies generated in the irradiation process [19,20]. The main goal of the present work is to overcome this limitation; thus, we first create perfectly characterized single vacancies on a graphite surface by Ar^+ ion irradiation and then, using low temperature scanning tunneling microscopy (LT-STM), we individually investigate the impact of each of such vacancies in the electronic and magnetic properties of this gra-

phenelike system. We identify well-localized electronic resonances at the Fermi energy around graphite single lattice vacancies. The existence of these states is in good agreement with theoretical expectations, and it can be associated with the formation of magnetic moments in this all-carbon material. Using simple extensions of these models, as well as the similarities between the properties of a clean graphite surface and single layer and multilayered graphene, we can extrapolate our results to those systems. In addition, we also show that contrary to the single layer graphene case, ferrimagnetism is favored in multilayered graphene samples.

We use highly ordered pyrolytic graphite (HOPG) samples, which present the AB Bernal stacking. Thus, one atom of the honeycomb unit cell (α) is located directly above a C atom of the second layer and the other one (β) is on top of a hollow site [see Fig. 1(b)]. A key point of the present work is the atomistic control of the samples, which was obtained by performing all the preparation procedures and measurements under UHV conditions. We created single vacancies by irradiating with 140 eV Ar^+ ions previously *in situ* exfoliated HOPG surfaces. At these low ion energies, just above the threshold value for the displacement of surface atoms, the ion irradiation mainly produces atomic point defects [19,20]. After further sample annealing at 650 °C, the remaining defects were mostly single vacancies as revealed by STM images. Figure 1(a) shows the general morphology of our samples after the irradiation and annealing procedure. The previous perfect and pristine graphite surface, now presents several point defects surrounded by threefold ($\sqrt{3} \times \sqrt{3}$) patterns, $R3$ in the following (see Fig. S1 in the supplemental material [21] for a more general overview). The comparison of our atomically resolved STM images of these defects [Figs. 1(a) and 1(c)] with calculations [22,23] shows that these defects correspond to single vacancies on both α and β sites of the graphite honeycomb lattice.

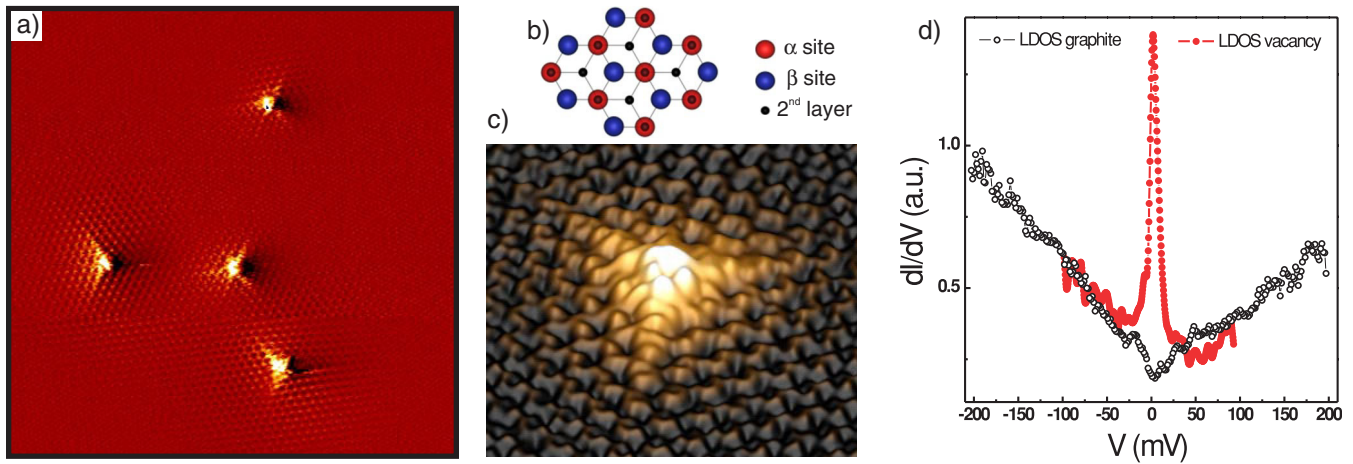


FIG. 1 (color online). (a) $17 \times 17 \text{ nm}^2$ STM topography, measured at 6 K, showing the graphite surface after the Ar^+ ion irradiation (for a larger scale overview of the same region, see [21]). Data analyzed using WSXM [37]. Single vacancies occupy both α and β sites of the graphite honeycomb lattice. Sample bias: +270 mV, tunneling current: 1 nA. (b) Schematic diagram of the graphite structure. (c) 3D view of a single isolated vacancy. Sample bias: +150 mV, tunneling current: 0.5 nA. (d) STS measurements of the LDOS induced by the single vacancy and of graphite. Black open circles correspond to dI/dV spectra measured on pristine graphite and red solid circles correspond to dI/dV spectra measured on top of the single vacancy, showing the appearance of a sharp resonance at E_F . dI/dV measurements were done consecutively at 6 K with the same microscopic tip.

We use a homemade LT-STM [24] to investigate the local electronic structure of the single atomic vacancies created in graphite. This is an unrivaled technique to provide local information about the surface electronic properties, achieving atomic precision and very high energy resolution ($\sim 1 \text{ meV}$ at 4.2 K). The use of these unique capabilities in graphenelike systems has already made it possible, for example, to detect the coexistence of both massless and massive Dirac fermions in a graphite surface [25,26], or to prove the Dirac nature of the quasiparticles in epitaxial graphene on SiC [27,28]. Differential conductance (dI/dV) spectra were measured in open feedback loop mode using the lock-in technique with frequency 2.3 kHz and ac modulation of 1 mV. Various tungsten (W) tips were used for the measurements. In order to avoid tip artifacts, tip status was always checked by measuring reference spectra on pristine graphite; only tips showing the standard featureless V-shaped spectra and a work function of 4–5 eV were considered in this work. Spectra remained unchanged for moderate tip-sample distance variations (stabilization current was routinely modified from 10 pA to 10 nA). Figure 1(d) shows consecutive dI/dV spectra, measured at 6 K, summarizing our results. Far enough from any defect, spectra showed a featureless V-shaped form as expected for the LDOS of pristine graphite (black circles). Spectra acquired on top of a single vacancy (red circles), both in α and β positions reveal the existence of a sharp resonance peak around the Fermi level (E_F) with a FWHM of $\sim 5 \text{ mV}$. The spatial localization of the resonance is shown in Fig. 2.

The presence of this resonance is a fundamental result that, although anticipated in many theoretical works, had never been experimentally observed before. The formation

of a magnetic moment can be associated to the resonance, since electron-electron interactions, and the fact that the localized level is very close to the Fermi energy, favor the polarization of this state. In addition, the narrowness of the resonance and the low electronic density of graphite at the Fermi level imply a very poor screening of the magnetic

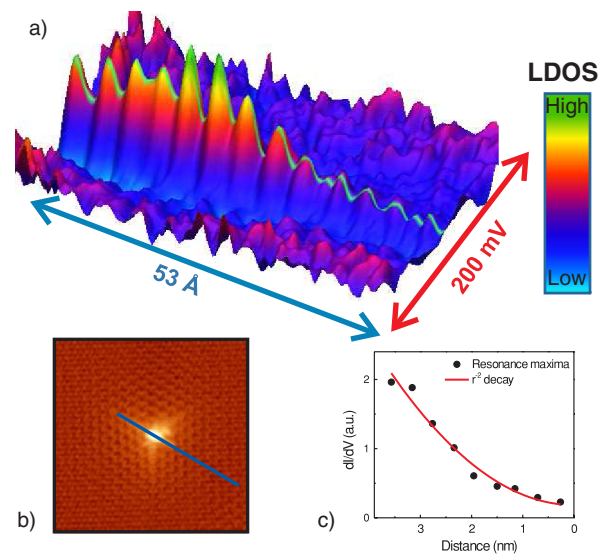


FIG. 2 (color online). (a) LDOS as a function of sample voltage V and position x along the line drawn in (b). A light central line has been drawn to outline the evolution of the resonance peak height, showing a clear R_3 modulation. (b) STM topographic image of a single graphite vacancy. Image size $8 \times 8 \text{ nm}^2$; sample bias +200 mV tunneling current 0.6 nA. (c) r^{-2} decay of the resonance intensity. Black dots correspond to the maxima of the resonance peak height and the line is parabolic fit to the experimental data.

moment, which anticipates a very high Curie temperature for the vacancies (see below). Our results also demonstrate that the presence of these single vacancies should have a strong impact on the electronic transport, since the existence of a resonance in the vicinity of the Fermi level gives rise to a strong reduction of the mobility, with a mean free path which tends to the distance between impurities at the neutrality point [29]. In this way, the artificial introduction of a chosen density of vacancies can be used as an effective method to tune the mobility of graphite and graphenelike samples.

The existence of this sharp resonance at the neutrality point in single layer graphene can be derived from the nearest neighbor tight-binding Hamiltonian which describes the π bands [7], neglecting deformations near the vacancy. We have checked that the resonance is also present in a semi-infinite graphite layer by extending the calculation and using the Slonczewski-Weiss-McClure parametrization of the π bands, which is expected to describe well the electronic structure near the Fermi level [30–32]. Results are shown in Fig. 3(b). Details of the calculation are given in the supporting material [21]. The results are consistent with those in Ref. [7], and with extensions of that model to multilayered graphene [33]. A sharp resonance exists when the vacancy is at α sites, while a lower peak is found near vacancies at β sites. The wave function Ψ associated to this resonance is very extended, decaying as a function of the distance to the vacancy as r^{-1} [6,33]. It shows a $R3$ modulation, associated to the wave vector which spans the two valleys in the Brillouin zone [21].

We have also analyzed experimentally the spatial extension of the states induced around single vacancies by

mapping the narrow resonance as a function of distance from the defect. Figure 2(a) shows a map of the local density of states (LDOS) vs energy, measured along the line across the vacancy drawn in Fig. 2(b). The narrow resonance extends several nanometers away from the vacancy, indicating that it is indeed a quasilocized state. The resonance shows an overall decreasing intensity with increasing distance, consistent with the expected r^{-1} decay (STM probes $|\Psi|^2$) as shown in Fig. 2(c), its height is modulated with the $R3$ periodicity [Fig. 2(a)] and its width remains approximately constant for all distances.

The agreement between the experimental results and the theoretical model shows that the latter describes correctly the main electronic properties of the vacancy. Electron-electron interactions prevent double occupancy of the resonance, and lead to the formation of a magnetic moment near the vacancy. The resonance is built up from π orbitals, and it is orthogonal to the extended states. Hence, the coupling between the magnetic moment and the conduction and valence bands is not due to virtual transitions involving short lived zero or doubly occupied states. These are the processes which describe the antiferromagnetic Kondo coupling induced by a magnetic impurity hybridized with a metallic band. In our case, we expect a ferromagnetic coupling mediated by the Coulomb repulsion [21]. Moreover, the magnetic moment is extended throughout many lattice cells around the vacancy, so that it interacts with many partial wave channels built up from the extended states, leading to a multichannel ferromagnetic Kondo system [34]. The magnetic moment is not quenched at low temperatures.

The interaction between magnetic moments induced by vacancies at different sites has been extensively studied for single layer graphene [8,9,35]. Its sign depends on the sublattice occupied by the vacancies. In graphite, the two sublattices are inequivalent. Our samples present vacancies in both α and β sites of the honeycomb lattice, which gives rise to two $R3$ scattering patterns of different shape and extension [21]. It is then natural to think that the quasilocized resonance, and thus the magnetic moment, induced by graphite single vacancies are also affected by the underlying C layers. Our dI/dV spectra clearly demonstrate that this is indeed the case. Figure 3(a) shows consecutive spectra measured, with exactly the same microscopic STM tip, on both types of vacancies and on clean graphite. A sharp resonance of very similar width (FWHM of ~ 5 mV) is induced by both types of vacancies; however, the intensity is much higher in the case of the α vacancy, in agreement with our calculations [Fig. 3(b)]. This inequivalence in the magnetic moment induced by each type of vacancy will reduce antiferromagnetic coupling, inhibiting complete frustration. Hence, we expect a ferrimagnetic ground state at low temperatures. The fact that the resonances form a narrow band of delocalized states suppresses screening effects and fluctuations due to spin waves [36]. A simple estimate based on the direct exchange coupling between moments localized around impurities gives a

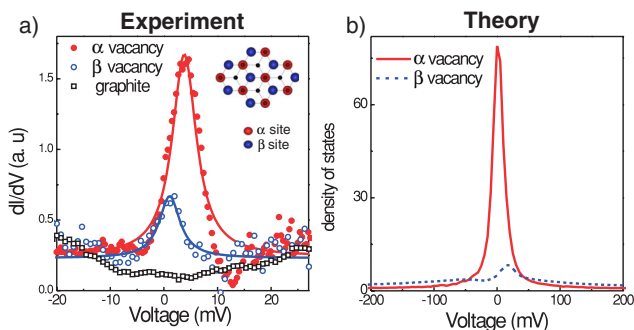


FIG. 3 (color online). (a) (dI/dV) spectra measured with the same tip on top of a single vacancy in an α (red solid circles), β (blue open circles) site and on pristine graphite (black squares). The intensity of the resonance measured on top of the α vacancy is much higher than the one of the β one, indicating that removing a C atom from an α site generates a stronger magnetic moment. Solid lines are fits to a Lorentzian function giving a FWHM of ~ 5 mV for both the resonance on the α and β site. Small variations (of a couple of mV) in the position of the resonance peak maxima were observed, which we attribute to the local environment of each specific vacancy. (b) Calculated density of states in the atom nearest to vacancy. Red solid line: vacancy in α site; blue dashed line: vacancy in β site.

Curie temperature $T_c \sim e^2 \sqrt{n_v}$, where e^2 is the electric charge ($\sim 1-5$ eV \cdot Å), and n_v is the vacancy concentration. In the present experiment, $n_v \sim 3 \times 10^{11}$ cm $^{-2}$ and this simple estimation suggest a Curie temperature $T_c \sim 50-200$ K [21].

Our findings have strong implications both from an applied and a fundamental point of view. They provide a significant stimulus to the theoretical community demonstrating that for atomistically controlled experiments, tight-binding methods give an excellent description of graphenelike systems physics. The observed resonances indicate that vacancies should limit significantly the mobility of carriers in graphene, and enhance its chemical reactivity. The existence of sharp electronic resonances at the Fermi energy strongly suggests the formation of magnetic moments around single vacancies in graphite surfaces, implying a magnetic phase for this free of impurities carbon system with high Curie temperatures and small magnetization moments, which indicates a suitable route to the creation of nonmetallic, cheaper, lighter, and biocompatible magnets.

We are thankful to J. Y. Veuillen and P. Mallet for providing us with the sputtering parameters. I. B was supported by a Ramón y Cajal project of the Spanish MEC. M. M. U. acknowledges financial support from MEC under FPU Grant No. AP-2004-1896. Financial support from Spain's MEC under Grants No. MAT2007-60686, FIS2008-00124, and CONSOLIDER CSD2007-00010, from the 7th European Community Framework Programme by a Marie Curie European Reintegration Grant and by the Comunidad de Madrid, through CITECNOMIK and through Grant No. S2009/MAT-1467, is gratefully acknowledged.

*Corresponding author.

ivan.brihuega@uam.es

- [1] N. B. Brandt, S. M. Chudinov, and Y. G. Ponomarev, *Modern Problems in Condensed Matter Sciences* (North Holland, Amsterdam, 1988), Vol. 20.1.
- [2] K. S. Novoselov *et al.*, *Science* **306**, 666 (2004).
- [3] K. S. Novoselov *et al.*, *Proc. Natl. Acad. Sci. U.S.A.* **102**, 10451 (2005).
- [4] M. Fujita, K. Wakabayashi, K. Nakada, and K. Kusakabe, *J. Phys. Soc. Jpn.* **65**, 1920 (1996).
- [5] T. Enoki, Y. Kobayashi, and K. I. Fukui, *Int. Rev. Phys. Chem.* **26**, 609 (2007).
- [6] V. M. Pereira, F. Guinea, J. M. Lopes dos Santos, N. M. R. Peres, and A. H. Castro Neto, *Phys. Rev. Lett.* **96**, 036801 (2006).
- [7] P. O. Lehtinen, A. S. Foster, Y. C. Ma, A. V. Krasheninnikov, and R. M. Nieminen, *Phys. Rev. Lett.* **93**, 187202 (2004).
- [8] O. V. Yazyev, *Phys. Rev. Lett.* **101**, 037203 (2008).
- [9] J. J. Palacios, J. Fernández-Rossier, and L. Brey, *Phys. Rev. B* **77**, 195428 (2008).
- [10] Y. Niimi *et al.*, *Phys. Rev. B* **73**, 085421 (2006).
- [11] Y. Shibayama, H. Sato, T. Enoki, and M. Endo, *Phys. Rev. Lett.* **84**, 1744 (2000).
- [12] K. Harigaya and T. Enoki, *Chem. Phys. Lett.* **351**, 128 (2002).
- [13] J. Cervenka, M. I. Katsnelson, and C. F. J. Flipse, *Nature Phys.* **5**, 840 (2009).
- [14] P. Esquinazi *et al.*, *Phys. Rev. Lett.* **91**, 227201 (2003).
- [15] H. Ohldag *et al.*, *Phys. Rev. Lett.* **98**, 187204 (2007).
- [16] A. V. Krasheninnikov and F. Banhart, *Nature Mater.* **6**, 723 (2007).
- [17] C. Gomez-Navarro *et al.*, *Nature Mater.* **4**, 534 (2005).
- [18] A. H. Castro Neto, F. Guinea, N. M. R. Peres, K. S. Novoselov, and A. K. Geim, *Rev. Mod. Phys.* **81**, 109 (2009).
- [19] A. Hashimoto, K. Suenaga, A. Gloter, K. Urita, and S. Iijima, *Nature (London)* **430**, 870 (2004).
- [20] J. R. Hahn and H. Kang, *Phys. Rev. B* **60**, 6007 (1999).
- [21] See supplementary material at <http://link.aps.org/supplemental/10.1103/PhysRevLett.104.096804> for a large sample overview and for details of the theoretical model.
- [22] H. A. Mizes and J. S. Foster, *Science* **244**, 559 (1989).
- [23] K. F. Kelly and N. J. Halas, *Surf. Sci.* **416**, L1085 (1998).
- [24] M. M. Ugeda, doctoral thesis, Universidad Autónoma de Madrid (to be published).
- [25] T. Matsui *et al.*, *Phys. Rev. Lett.* **94**, 226403 (2005).
- [26] G. Li and E. Y. Andrei, *Nature Phys.* **3**, 623 (2007).
- [27] I. Brihuega *et al.*, *Phys. Rev. Lett.* **101**, 206802 (2008).
- [28] D. L. Miller *et al.*, *Science* **324**, 924 (2009).
- [29] T. Stauber, N. M. R. Peres, and F. Guinea, *Phys. Rev. B* **76**, 205423 (2007).
- [30] D. P. Arovas and F. Guinea, *Phys. Rev. B* **78**, 245416 (2008).
- [31] J. C. Slonczewski and P. R. Weiss, *Phys. Rev.* **109**, 272 (1958).
- [32] J. W. McClure, *Phys. Rev.* **108**, 612 (1957).
- [33] E. V. Castro, M. P. López-Sancho, and M. A. H. Vozmediano, *Phys. Rev. Lett.* **104**, 036802 (2010).
- [34] A. C. Hewson, *The Kondo Problem to Heavy Fermions* (Cambridge University Press, Cambridge, 1993).
- [35] L. Brey, H. A. Fertig, and S. Das Sarma, *Phys. Rev. Lett.* **99**, 116802 (2007).
- [36] D. M. Edwards and M. I. Katsnelson, *J. Phys. Condens. Matter* **18**, 7209 (2006).
- [37] I. Horcas *et al.*, *Rev. Sci. Instrum.* **78**, 013705 (2007).